PERGAMON

International Journal of Solids and Structures 40 (2003) 105–123

INTERNATIONAL JOURNAL OF SOLIDS and STRUCTURES

www.elsevier.com/locate/ijsolstr

The transient responses of piezoelectric hollow cylinders for axisymmetric plane strain problems

H.J. Ding [a,*], H.M. Wang [b], P.F. Hou [c]

[a] *Department of Civil Engineering, Zhejiang University, Hangzhou 310027, PR China*
[b] *Department of Engineering Mechanics, Zhejiang University, Hangzhou 310027, PR China*
[c] *Department of Engineering Mechanics, Hunan University, Changsha 410082, PR China*

Received 26 December 2001; received in revised form 16 September 2002

Abstract

By virtue of the separation of variables technique, the axisymmetric plane strain electroelastic dynamic problem of hollow cylinder is transferred to an integral equation about a function with respect to time, which can be solved successfully by means of the interpolation method. Then the solution of the displacements, stresses, electric displacements and electric potentials are finally obtained. The present method is suitable for the hollow cylinder with arbitrary thickness subjected to arbitrary mechanical and electrical loads. Numerical results are also presented.

Keywords: Piezoelectric; Hollow cylinder; Axisymmetric; Electroelastic; Dynamic

1. Introduction

The analyses for dynamic problems of elastic bodies are important and interesting research fields for engineers and scientists. Being the common structural form, the hollow cylinders (cylindrical shells) are studied extensively. For non-piezoelectric media, based on the momentless thin shell theory, Mcivor (1966) discussed the flexural stresses and membrane stresses in an elastic cylindrical shell under an arbitrary impulsive pressure distribution. Using the method of characteristics, the dynamic responses of cylindrical and spherical shells were studied by Chou and Koenig (1966) and Rose et al. (1973). By means of the finite Hankel transform and Laplace transform, Cinelli (1966) obtained the theoretical solutions of cylindrical and spherical shells. Wang and Gong (1991) studied the stress responses of isotropic cylindrical shells shocked at the inner surface. While for piezoelectric media, Adelman and Stavsky (1975) studied the axisymmetric free vibrations of radially polarized piezoelectric ceramic hollow cylinders. The torsional wave motion of a finite inhomogeneous piezoelectric cylindrical shell was solved by Sarma (1980), in which the

* Corresponding author. Tel.: +86-571-8795-2267; fax: +86-571-8795-2165.
E-mail addresses: hjding@mail.hz.zj.cn (H.J. Ding), wanghuiming@cmee.zju.edu.cn (H.M. Wang).

0020-7683/02/$ - see front matter
PII: S0020-7683(02)00525-5

material constants are assumed to vary as the $2N$th power of r and the boundary conditions were time dependent, axisymmetric electric potentials. It's noted that the solution is only fit for class 622 crystals but not fit for class 6 mm crystals. Shul'ga et al. (1984) investigated the axisymmetric electroelastic waves in a hollow piezoelectric ceramic cylinder. The free vibrations of piezoelectric, empty and also compressible fluid filled cylindrical shells for three-dimensional problems were studied by Ding et al. (1997a,b). Comparing with non-piezoelectric media, it is more difficult to obtain the dynamic analytical solution because of the special coupling effect between mechanical deformation and electrical field. At present, the most works are located to study the fields of free vibrations and wave propagations. While the transient responses, although they are very important, have not been studied to the author's knowledge.

In this paper, a method is developed for solving the transient response of axisymmetric plane strain problem of piezoelectric hollow cylinders subjected to dynamic loads. Firstly, a special function is introduced to transform the inhomogeneous mechanical boundary conditions into the homogeneous ones. Secondly, by virtue of the orthogonal expansion technique and by using the initial conditions as well as electrical boundary conditions, the integral equation about a function with respect to time is then derived, which is possible to be solved by means of interpolation method. And finally, the displacement, stresses, electric displacement and electric potential are obtained. The present method is suitable for the hollow cylinder with arbitrary thickness subjected to arbitrary mechanical and electrical loads. The transient responses of piezoelectric hollow cylinders subjected to a suddenly constant pressure on the internal surface and a suddenly constant electric potential on the external surface are completed.

2. Basic formulations

In cylindrical coordinates (r,θ,z), for the axisymmetric problem, the components of displacement and electric potential satisfy $u_\theta = 0$, $u_r = u_r(r,z,t)$, $u_z = u_z(r,z,t)$ and $\Phi = \Phi(r,z,t)$, respectively. If it is further a plane strain problem, we get $u_\theta = u_z = 0$, $u_r = u_r(r,t)$ and $\Phi = \Phi(r,t)$. In this case, the strain-displacement relations are simplified

$$\gamma_{rr} = \frac{\partial u_r}{\partial r}, \quad \gamma_{\theta\theta} = \frac{u_r}{r}, \tag{1}$$

where γ_{ij} are the strain components. The constitutive relations of orthotropic, radially polarized piezoelectric media are

$$\begin{aligned}
\sigma_{\theta\theta} &= c_{11}\gamma_{\theta\theta} + c_{13}\gamma_{rr} + e_{31}\frac{\partial \Phi}{\partial r},\\
\sigma_{zz} &= c_{12}\gamma_{\theta\theta} + c_{23}\gamma_{rr} + e_{32}\frac{\partial \Phi}{\partial r},\\
\sigma_{rr} &= c_{13}\gamma_{\theta\theta} + c_{33}\gamma_{rr} + e_{33}\frac{\partial \Phi}{\partial r},\\
D_r &= e_{31}\gamma_{\theta\theta} + e_{33}\gamma_{rr} - \varepsilon_{33}\frac{\partial \Phi}{\partial r},
\end{aligned} \tag{2}$$

where c_{ij}, e_{ij} and ε_{ij} are elastic constants, piezoelectric constants and dielectric constants, respectively. σ_{ij} and D_r are the components of stress and radial electric displacement, respectively. The equation of motion is

$$\frac{\partial \sigma_{rr}}{\partial r} + \frac{\sigma_{rr} - \sigma_{\theta\theta}}{r} = \rho\frac{\partial^2 u_r}{\partial t^2}, \tag{3}$$

where ρ is the mass density. In order to show the results, the following non-dimensional forms are introduced,

$$c_1=\frac{c_{11}}{c_{33}},\quad c_2=\frac{c_{12}}{c_{33}},\quad c_3=\frac{c_{13}}{c_{33}},\quad c_4=\frac{c_{23}}{c_{33}},\quad e_1=\frac{e_{31}}{\sqrt{c_{33}\varepsilon_{33}}},\quad e_2=\frac{e_{32}}{\sqrt{c_{33}\varepsilon_{33}}},$$
$$e_3=\frac{e_{33}}{\sqrt{c_{33}\varepsilon_{33}}},\quad \sigma_i=\frac{\sigma_{ii}}{c_{33}}(i=r,\theta,z),\quad \phi=\sqrt{\frac{\varepsilon_{33}}{c_{33}}}\frac{\Phi}{b},\quad D=\frac{D_r}{\sqrt{c_{33}\varepsilon_{33}}},\quad u=\frac{u_r}{b}, \tag{4}$$
$$\xi=\frac{r}{b},\quad s=\frac{a}{b},\quad c_v=\sqrt{\frac{c_{33}}{\rho}},\quad \tau=\frac{c_v}{b}t,$$

where a and b are the inner and outer radii of hollow cylinder, respectively. Then Eqs. (1)–(3) can be rewritten as follows:

$$\gamma_{rr}=\frac{\partial u}{\partial\xi},\quad \gamma_{\theta\theta}=\frac{u}{\xi}, \tag{5}$$

$$\sigma_\theta=c_1\frac{u}{\xi}+c_3\frac{\partial u}{\partial\xi}+e_1\frac{\partial\phi}{\partial\xi},\quad \sigma_z=c_2\frac{u}{\xi}+c_4\frac{\partial u}{\partial\xi}+e_2\frac{\partial\phi}{\partial\xi},$$
$$\sigma_r=c_3\frac{u}{\xi}+\frac{\partial u}{\partial\xi}+e_3\frac{\partial\phi}{\partial\xi},\quad D=e_1\frac{u}{\xi}+e_3\frac{\partial u}{\partial\xi}-\frac{\partial\phi}{\partial\xi}, \tag{6}$$

$$\frac{\partial\sigma_r}{\partial\xi}+\frac{\sigma_r-\sigma_\theta}{\xi}=\frac{\partial^2u}{\partial\tau^2}. \tag{7}$$

In absence of free charge density, the charge equation of electrostatics is

$$\frac{1}{\xi}\frac{\partial}{\partial\xi}(\xi D)=0. \tag{8}$$

The boundary conditions are

$$\sigma_r(s,\tau)=p_a(\tau),\quad \sigma_r(1,\tau)=p_b(\tau), \tag{9a}$$

$$\phi(s,\tau)=\phi_a(\tau),\quad \phi(1,\tau)=\phi_b(\tau), \tag{9b}$$

where $p_a(\tau)$ and $p_b(\tau)$ are known nondimensional pressures subjected to the internal and external surfaces of the hollow cylinder, respectively. And $\phi_a(\tau)$ and $\phi_b(\tau)$ are known nondimensional electric potentials subjected to the internal and external surfaces of the hollow cylinder, respectively.

The initial conditions are expressed as

$$\tau=0: u(\xi,0)=u_0(\xi),\quad \dot{u}(\xi,0)=v_0(\xi), \tag{10}$$

where a dot over a quantity denotes its partial derivative with respect to time.

3. Solving technology

At first, we rewrite the fourth equation in Eq. (6) as

$$\frac{\partial\phi}{\partial\xi}=e_1\frac{u}{\xi}+e_3\frac{\partial u}{\partial\xi}-D. \tag{11}$$

Then substituting Eq. (11) into the first three equations in Eq. (6), gives

$$\sigma_\theta=c_1^D\frac{u}{\xi}+c_3^D\frac{\partial u}{\partial\xi}-e_1D,\quad \sigma_z=c_2^D\frac{u}{\xi}+c_4^D\frac{\partial u}{\partial\xi}-e_2D,\quad \sigma_r=c_3^D\frac{u}{\xi}+c_0^D\frac{\partial u}{\partial\xi}-e_3D, \tag{12}$$

where

$$c_1^D = c_1 + e_1^2, \quad c_2^D = c_2 + e_1 e_2, \quad c_3^D = c_3 + e_1 e_3, \quad c_4^D = c_4 + e_2 e_3, \quad c_0^D = 1 + e_3^2. \tag{13}$$

From Eq. (8), we get

$$D(\xi,\tau) = \frac{1}{\xi} d(\tau), \tag{14}$$

where $d(\tau)$ is an unknown function with respect to nondimensional time τ. Substituting the first and the third equations in Eq. (12) into Eq. (7), and utilizing Eq. (14), derives

$$\frac{\partial^2 u}{\partial \xi^2} + \frac{1}{\xi}\frac{\partial u}{\partial \xi} - \frac{\mu^2}{\xi^2} u = \frac{1}{c_L^2}\frac{\partial^2 u}{\partial \tau^2} - \frac{e_1}{c_0^D}\frac{1}{\xi^2} d(\tau), \tag{15}$$

where

$$\mu = \sqrt{\frac{c_1^D}{c_0^D}}, \quad c_L = \sqrt{c_0^D}. \tag{16}$$

Utilizing the third equation in Eq. (12) and Eq. (14), we can rewrite Eq. (9a) as

$$\xi = s : \frac{\partial u}{\partial \xi} + h\frac{u}{\xi} = p_1(\tau), \quad \xi = 1 : \frac{\partial u}{\partial \xi} + h\frac{u}{\xi} = p_2(\tau), \tag{17}$$

where

$$h = \frac{c_3^D}{c_0^D}, \quad p_1(\tau) = \frac{1}{c_0^D}\left[p_a(\tau) + \frac{e_3}{s} d(\tau)\right], \quad p_2(\tau) = \frac{1}{c_0^D}[p_b(\tau) + e_3 d(\tau)]. \tag{18}$$

Next, a new variable $w_1(\xi,\tau)$ is introduced to rewrite the inhomogeneous boundary conditions (17) which are expressed by radial displacement $u(\xi,\tau)$ by assuming

$$u(\xi,\tau) = w_1(\xi,\tau) + w_2(\xi,\tau), \tag{19}$$

where $w_2(\xi,\tau)$ satisfies the inhomogeneous boundary conditions (17) and can be taken as

$$w_2(\xi,\tau) = A_0(\xi - s)^m p_2(\tau) + B_0(\xi - 1)^m p_1(\tau), \tag{20}$$

in which

$$A_0 = \frac{1}{m(1-s)^{m-1} + h(1-s)^m}, \quad B_0 = \frac{1}{m(s-1)^{m-1} + h(s-1)^m/s}, \tag{21}$$

here m is an arbitrary integer, which is no less than 2, and should satisfy

$$[m(1-s)^{m-1} + h(1-s)^m][m(s-1)^{m-1} + h(s-1)^m/s] \neq 0. \tag{22}$$

Substituting Eq. (18) into Eq. (20), $w_2(\xi,\tau)$ can be rewritten as

$$w_2(\xi,\tau) = f_1(\xi)p_a(\tau) + f_2(\xi)p_b(\tau) + f_3(\xi)\, d(\tau), \tag{23}$$

where

$$f_1(\xi) = \frac{B_0}{c_0^D}(\xi - 1)^m, \quad f_2(\xi) = \frac{A_0}{c_0^D}(\xi - s)^m, \quad f_3(\xi) = e_3\left[\frac{1}{s} f_1(\xi) + f_2(\xi)\right]. \tag{24}$$

Substituting Eq. (19) into Eqs. (15), (17) and (10), yields

$$\frac{\partial^2 w_1(\xi,\tau)}{\partial\xi^2}+\frac{1}{\xi}\frac{\partial w_1(\xi,\tau)}{\partial\xi}-\frac{\mu^2}{\xi^2}w_1(\xi,\tau)=\frac{1}{c_L^2}\frac{\partial^2 w_1(\xi,\tau)}{\partial\tau^2}+g(\xi,\tau), \tag{25}$$

$$\frac{\partial w_1(\xi,\tau)}{\partial\xi}+h\frac{w_1(\xi,\tau)}{\xi}=0,\quad (\xi=s,1), \tag{26}$$

$$w_1(\xi,0)=u_0(\xi)-w_2(\xi,0),\quad \dot{w}_1(\xi,0)=v_0(\xi)-\dot{w}_2(\xi,0), \tag{27}$$

where

$$g(\xi,\tau)=\frac{1}{c_L^2}\frac{\partial^2 w_2(\xi,\tau)}{\partial\tau^2}+\frac{\mu^2}{\xi^2}w_2(\xi,\tau)-\frac{1}{\xi}\frac{\partial w_2(\xi,\tau)}{\partial\xi}-\frac{\partial^2 w_2(\xi,\tau)}{\partial\xi^2}-\frac{e_1}{c_0^D}\frac{1}{\xi^2}d(\tau). \tag{28}$$

Substituting Eq. (23) into Eq. (28), derives

$$g(\xi,\tau)=g_1(\xi,\tau)+g_2(\xi)\,\mathrm{d}(\tau)+g_3(\xi)\ddot{\boldsymbol{d}}(\tau), \tag{29}$$

where

$$\begin{aligned}
&g_1(\xi,\tau)=f_4(\xi)p_a(\tau)+f_5(\xi)p_b(\tau)+\frac{1}{c_L^2}[f_1(\xi)\ddot{p}_a(\tau)+f_2(\xi)\ddot{p}_b(\tau)],\\
&g_2(\xi)=\frac{\mu^2}{\xi^2}f_3(\xi)-\frac{1}{\xi}\frac{\mathrm{d}f_3(\xi)}{\mathrm{d}\xi}-\frac{\mathrm{d}^2 f_3(\xi)}{d\xi^2}-\frac{e_1}{c_0^D}\frac{1}{\xi^2},\quad g_3(\xi)=\frac{f_3(\xi)}{c_L^2},\\
&f_4(\xi)=\frac{\mu^2}{\xi^2}f_1(\xi)-\frac{1}{\xi}\frac{\mathrm{d}f_1(\xi)}{\mathrm{d}\xi}-\frac{\mathrm{d}^2 f_1(\xi)}{\mathrm{d}\xi^2},\\
&f_5(\xi)=\frac{\mu^2}{\xi^2}f_2(\xi)-\frac{1}{\xi}\frac{\mathrm{d}f_2(\xi)}{\mathrm{d}\xi}-\frac{\mathrm{d}^2 f_2(\xi)}{\mathrm{d}\xi^2}.
\end{aligned} \tag{30}$$

Using the separation of variables method, the solution of Eq. (25) can be assumed as

$$w_1(\xi,\tau)=\sum_i R_i(\xi)F_i(\tau), \tag{31}$$

where $F_i(\tau)$ is an undetermined function and $R_i(\xi)$ is given as follows

$$R_i(\xi)=J_\mu(k_i\xi)Y(\mu,k_i,s)-Y_\mu(k_i\xi)J(\mu,k_i,s), \tag{32}$$

where $J_\mu(k_i\xi)$ and $Y_\mu(k_i\xi)$ are Bessel functions of the first and second kinds of order μ. And k_i, arranged in an ascending order, are a series of positive roots of the following eigenequation

$$J(\mu,k_i,s)Y(\mu,k_i,1)-J(\mu,k_i,1)Y(\mu,k_i,s)=0, \tag{33}$$

where

$$J(\mu,k_i,\xi)=\frac{\mathrm{d}J_\mu(k_i\xi)}{\mathrm{d}\xi}+h\frac{J_\mu(k_i\xi)}{\xi},\quad Y(\mu,k_i,\xi)=\frac{\mathrm{d}Y_\mu(k_i\xi)}{\mathrm{d}\xi}+h\frac{Y_\mu(k_i\xi)}{\xi}. \tag{34}$$

It can be shown that $w_1(\xi,\tau)$ given in Eq. (31) satisfies the homogeneous boundary conditions in Eq. (26). Substituting Eq. (31) into Eq. (25) gives

$$-c_L^2\sum_i k_i^2F_i(\tau)R_i(\xi)=\sum_i R_i(\xi)\frac{\mathrm{d}^2F_i(\tau)}{\mathrm{d}\tau^2}+c_L^2g(\xi,\tau). \tag{35}$$

By virtue of the orthogonal properties of Bessel functions, it is easy to verify that $R_i(\xi)$ has the following properties

$$\int_s^1 \xi R_i(\xi) R_j(\xi)\,\mathrm{d}\xi = N_i \delta_{ij}, \tag{36}$$

where δ_{ij} is the Kronecker delta, and

$$N_i = \frac{1}{2k_i^2}\left\{\left[\frac{\mathrm{d}R_i(1)}{\mathrm{d}\xi}\right]^2 - s^2\left[\frac{\mathrm{d}R_i(s)}{\mathrm{d}\xi}\right]^2 + k_i^2\left[R_i^2(1) - s^2R_i^2(s)\right] - \mu^2\left[R_i^2(1) - R_i^2(s)\right]\right\}, \tag{37}$$

in which $\mathrm{d}R_i(s)/\mathrm{d}\xi = \mathrm{d}R_i(\xi)/\mathrm{d}\xi|_{\xi=s}$ and $\mathrm{d}R_i(1)/\mathrm{d}\xi = \mathrm{d}R_i(\xi)/\mathrm{d}\xi|_{\xi=1}$. Utilizing Eq. (36), we can derive the following equation from Eq. (35)

$$\frac{\mathrm{d}^2F_i(\tau)}{\mathrm{d}\tau^2} + \omega_i^2 F_i(\tau) = q_i(\tau), \tag{38}$$

where

$$\begin{aligned}
&q_i(\tau) = q_{1i}(\tau) + h_{1i}\,d(\tau) + h_{2i}\ddot{\boldsymbol{d}}(\tau),\\
&\omega_i = k_i c_L, \quad q_{1i}(\tau) = -c_L^2\int_s^1 \xi g_1(\xi,\tau) R_i(\xi)\,\mathrm{d}\xi/N_i,\\
&h_{1i} = -c_L^2\int_s^1 \xi g_2(\xi) R_i(\xi)\,\mathrm{d}\xi/N_i,\\
&h_{2i} = -c_L^2\int_s^1 \xi g_3(\xi) R_i(\xi)\,\mathrm{d}\xi/N_i.
\end{aligned} \tag{39}$$

The solution of Eq. (38) is

$$F_i(\tau) = H_{1i}\cos\omega_i\tau + \frac{H_{2i}}{\omega_i}\sin\omega_i\tau + \frac{1}{\omega_i}\int_0^\tau q_i(p)\sin\omega_i(\tau-p)\,\mathrm{d}p. \tag{40a}$$

We also can derive the following equation from Eq. (40a)

$$\dot{F}_i(\tau) = -\omega_i H_{1i}\sin\omega_i\tau + H_{2i}\cos\omega_i\tau + \int_0^\tau q_i(p)\cos\omega_i(\tau-p)\,\mathrm{d}p, \tag{40b}$$

where H_{1i} and H_{2i} are unknown constants. Using Eq. (23), the initial conditions in Eq. (27) can be rewritten as

$$w_1(\xi,0) = u_1(\xi) - f_3(\xi)\,d(0), \quad \dot{w}_1(\xi,0) = v_1(\xi) - f_3(\xi)\,\dot{\boldsymbol{d}}(0), \tag{41}$$

where

$$u_1(\xi) = u_0(\xi) - f_1(\xi)p_a(0) - f_2(\xi)p_b(0), \quad v_1(\xi) = v_0(\xi) - f_1(\xi)\dot{p}_a(0) - f_2(\xi)\dot{p}_b(0). \tag{42}$$

Utilizing Eq. (31), Eqs. (41) and (36), gives

$$H_{1i} = I_{1i} + I_{2i}\,d(0), \quad H_{2i} = I_{3i} + I_{2i}\,\dot{\boldsymbol{d}}(0), \tag{43}$$

where

$$I_{1i} = \frac{1}{N_i}\int_s^1 \xi u_1(\xi) R_i(\xi)\,\mathrm{d}\xi, \quad I_{2i} = -\frac{1}{N_i}\int_s^1 \xi f_3(\xi) R_i(\xi)\,\mathrm{d}\xi, \quad I_{3i} = \frac{1}{N_i}\int_s^1 \xi v_1(\xi) R_i(\xi)\,\mathrm{d}\xi. \tag{44}$$

Noticing that $\ddot{d}(\tau)$ is involved in $q_i(\tau)$ in Eqs. (40a) and (40b), we use the integration-by-parts formula and obtain

$$\int_0^\tau \ddot{d}(p)\sin\omega_i(\tau-p)\,\mathrm{d}p = -\dot{d}(0)\sin\omega_i\tau - d(0)\omega_i\cos\omega_i\tau + \omega_i d(\tau) - \omega_i^2\int_0^\tau d(p)\sin\omega_i(\tau-p)\,\mathrm{d}p. \tag{45}$$

Substituting the first equation in Eq. (39) into Eq. (40a) and utilizing Eq. (45), gives

$$F_i(\tau) = F_{1i}(\tau) + h_{2i}d(\tau) + \left(\frac{h_{1i}}{\omega_i} - h_{2i}\omega_i\right)\int_0^\tau d(p)\sin\omega_i(\tau-p)\,\mathrm{d}p, \tag{46}$$

where

$$F_{1i}(\tau) = H_{1i}\cos\omega_i\tau + \frac{H_{2i}}{\omega_i}\sin\omega_i\tau + \frac{1}{\omega_i}\int_0^\tau q_{1i}(p)\sin\omega_i(\tau-p)\,\mathrm{d}p - \frac{h_{2i}}{\omega_i}[\dot{d}(0)\sin\omega_i\tau + d(0)\omega_i\cos\omega_i\tau]. \tag{47}$$

In the following, we will determine $d(\tau)$ by means of the electric boundary conditions in Eq. (9b). Substituting Eq. (14) into Eq. (11), gives

$$\frac{\partial\phi}{\partial\xi} = e_1\frac{u}{\xi} + e_3\frac{\partial u}{\partial\xi} - \frac{1}{\xi}d(\tau). \tag{48}$$

Then substituting Eqs. (23) and (31) into Eq. (19), reads

$$u(\xi,\tau) = \sum_i R_i(\xi)F_i(\tau) + f_1(\xi)p_a(\tau) + f_2(\xi)p_b(\tau) + f_3(\xi)d(\tau). \tag{49}$$

Integrating Eq. (48) and utilizing Eq. (49), derives

$$\phi(\xi,\tau) = \phi_1(\xi)p_a(\tau) + \phi_2(\xi)p_b(\tau) + \phi_3(\xi)d(\tau) + \sum_i \phi_{4i}(\xi)F_i(\tau) + \phi_a(\tau), \tag{50}$$

where

$$\begin{aligned}
&\phi_1(\xi) = e_1\int_s^\xi \frac{f_1(\xi)}{\xi}\mathrm{d}\xi + e_3[f_1(\xi) - f_1(s)], \quad \phi_2(\xi) = e_1\int_s^\xi \frac{f_2(\xi)}{\xi}\mathrm{d}\xi + e_3[f_2(\xi) - f_2(s)],\\
&\phi_3(\xi) = e_1\int_s^\xi \frac{f_3(\xi)}{\xi}\mathrm{d}\xi + e_3[f_3(\xi) - f_3(s)] - \ln\left(\frac{\xi}{s}\right), \quad \phi_{4i}(\xi) = e_1\int_s^\xi \frac{R_i(\xi)}{\xi}\mathrm{d}\xi + e_3[R_i(\xi) - R_i(s)].
\end{aligned} \tag{51}$$

If $\xi = 1$, Eq. (50) read as

$$\phi_b(\tau) = \phi_1(1)p_a(\tau) + \phi_2(1)p_b(\tau) + \phi_3(1)d(\tau) + \sum_i \phi_{4i}(1)F_i(\tau) + \phi_a(\tau). \tag{52}$$

Then we have

$$\dot{\phi}_b(\tau) = \phi_1(1)\dot{p}_a(\tau) + \phi_2(1)\dot{p}_b(\tau) + \phi_3(1)\dot{d}(\tau) + \sum_i \phi_{4i}(1)\dot{F}_i(\tau) + \dot{\phi}_a(\tau). \tag{53}$$

If $\tau = 0$, we can determine $d(0)$ and $\dot{d}(0)$ without any difficulty from Eqs. (52) and (53) by using Eq. (40) and (43).

$$d(0) = \frac{\phi_b(0) - \phi_a(0) - \phi_1(1)p_a(0) - \phi_2(1)p_b(0) - \sum_i \phi_{4i}(1)I_{1i}}{\phi_3(1) + \sum_i \phi_{4i}(1)I_{2i}},$$
$$\dot{d}(0) = \frac{\dot{\phi}_b(0) - \dot{\phi}_a(0) - \phi_1(1)\dot{p}_a(0) - \phi_2(1)\dot{p}_b(0) - \sum_i \phi_{4i}(1)I_{3i}}{\phi_3(1) + \sum_i \phi_{4i}(1)I_{2i}}. \tag{54}$$

Substituting $d(0)$ and $\dot{d}(0)$ into Eq. (43) and Eq. (47), then H_{1i} and H_{2i} become known constants and $F_{1i}(\tau)$ become known functions. Substituting Eq. (46) into Eq. (52), derives

$$\psi(\tau) = E_1 d(\tau) + \sum_i E_{2i} \int_0^\tau d(p) \sin \omega_i(\tau - p)\,\mathrm{d}p, \tag{55}$$

where

$$\psi(\tau) = \phi_b(\tau) - \phi_a(\tau) - \phi_1(1)p_a(\tau) - \phi_2(1)p_b(\tau) - \sum_i \phi_{4i}(1)F_{1i}(\tau),$$
$$E_1 = \phi_3(1) + \sum_i \phi_{4i}(1)h_{2i}, \quad E_{2i} = \phi_{4i}(1)\left(\frac{h_{1i}}{\omega_i} - h_{2i}\omega_i\right). \tag{56}$$

It is noted that Eq. (55) is the Volterra integral equation of the second kind (Kress, 1989). We also know that the Eq. (55) has unique solution at all times. For some cases, the analytical solution can be obtained. While for general cases, numerical methods are needed. In this paper, we construct the recursion formula by making use of linear interpolation function. In practically, the numerical result can be obtained efficiently by the present method. In order to show the method of solving the integral equation, we first divide the time interval $[0, \tau_n]$ into n subintervals. The discrete time points are $\tau_0 = 0, \tau_1, \tau_2, \ldots, \tau_n$. Then the interpolation function at the time interval $[\tau_{j-1}, \tau_j]$ is

$$d(\tau) = \zeta_j(\tau) d(\tau_{j-1}) + \eta_j(\tau) d(\tau_j) \quad (j = 1, 2, \ldots, n), \tag{57}$$

where

$$\zeta_j(\tau) = \frac{\tau - \tau_j}{\tau_{j-1} - \tau_j}, \quad \eta_j(\tau) = \frac{\tau - \tau_{j-1}}{\tau_j - \tau_{j-1}} \qquad (j = 1, 2, \ldots, n). \tag{58}$$

Substituting Eq. (57) into Eq. (55), gives

$$\psi(\tau_j) = E_1 d(\tau_j) + \sum_i E_{2i} \sum_{k=1}^{j} [L_{ijk} d(\tau_{k-1}) + M_{ijk} d(\tau_k)], \tag{59}$$

where

$$L_{ijk} = \int_{\tau_{k-1}}^{\tau_k} \zeta_k(p) \sin \omega_i(\tau_j - p)\,\mathrm{d}p,$$
$$M_{ijk} = \int_{\tau_{k-1}}^{\tau_k} \eta_k(p) \sin \omega_i(\tau_j - p)\,\mathrm{d}p, \quad (k = 1, 2 \cdots j, \;\; j = 1, 2, \ldots, n). \tag{60}$$

Then we can derive the following formula from Eq. (59).

$$d(\tau_j) = \frac{\psi(\tau_j) - \sum_i E_{2i} \sum_{k=1}^{j-1} [L_{ijk} d(\tau_{k-1}) + M_{ijk} d(\tau_k)] - d(\tau_{j-1}) \sum_i E_{2i} L_{ijj}}{E_1 + \sum_i E_{2i} M_{ijj}}, \;\; (j = 1, 2, \ldots, n). \tag{61}$$

In Eq. (54), we have obtained $d(0)$. So we can obtain $d(\tau_j)$ $(j = 1, 2, \ldots, n)$ step by step. And $d(\tau)$ is then determined. Also $u(\xi, \tau)$ and $\phi(\xi, \tau)$ can be finally determined.

4. Numerical results and discussions

The transient responses of PZT-4 piezoelectric hollow cylinder subjected to a suddenly constant pressure and a sine time history pressure on the internal surface, as well as a suddenly constant electric potential and a electric potential varied with a sine time on the external surface are to be considered. The material constants (Dunn and Taya, 1994) are $c_{11} = c_{22} = 139.0$ GPa, $c_{12} = 77.8$ GPa, $c_{13} = c_{23} = 74.3$ GPa, $c_{33} = 115.0$ GPa, $e_{31} = e_{32} = -5.2$ (C/m^2), $e_{33} = 15.1$ (C/m^2), $\varepsilon_{33} = 5.62 \times 10^{-9}$ (C^2/N m^2). In order to compare with those in the non-piezoelectric hollow cylinder, we take the elastic constants of the non-piezoelectric media same as those of PZT-4 media. In the calculation that follows, we take $s = 0.5$, $m = 2$, $\tau_n = \tau_{200} = 10$ and the first 30 terms in Eq. (31).

Example 1. The transient responses in the hollow cylinder subjected to a suddenly constant pressure on the internal surface are to be considered. The boundary conditions are

$$p_a(\tau) = -\sigma_0 H(\tau), \quad p_b(\tau) = 0.0, \quad \phi_a(\tau) = 0.0, \quad \phi_b(\tau) = 0.0, \tag{62}$$

where σ_0 is a prescribed constant stress and we take $\sigma_0 = 1.0$ for computation. $H(\tau)$ means the Heaviside function.

Fig. 1 shows the responses of σ_r at $\xi = 0.75$ (the middle surface) in the PZT-4 and non-piezoelectric hollow cylinder due to an internal mechanical load shock. From the curves, we can see that the peak values of radial dynamic stresses in the PZT-4 hollow cylinder are larger than those in the non-piezoelectric one. And the response curves of the PZT-4 and the non-piezoelectric hollow cylinder are different with each other.

Figs. 2 and 3 give the responses of σ_θ at $\xi = 0.5$ (the internal surface) and $\xi = 1.0$ (the external surface) in the PZT-4 and the non-piezoelectric hollow cylinder. For PZT-4 hollow cylinder, we find that the maximum values of dynamic hoop stresses appear at the internal surface and it is tensile stress. The first peak value appears at the time $\tau = 2.40$ and it is 4.28 times of the amplitude of the step input. While for non-piezoelectric hollow cylinder, we also find that the maximum values of dynamic hoop stresses appear at the internal surface and it is tensile stress. The first peak value appears at the time $\tau = 2.45$, later than that

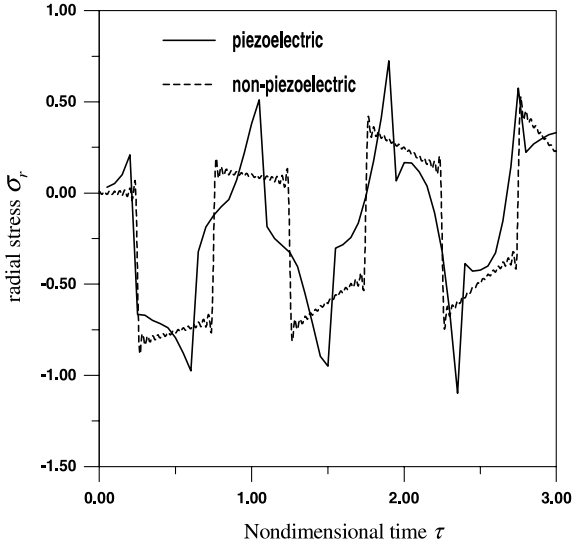

Fig. 1. History of dynamic stress σ_r at $\xi = 0.75$.

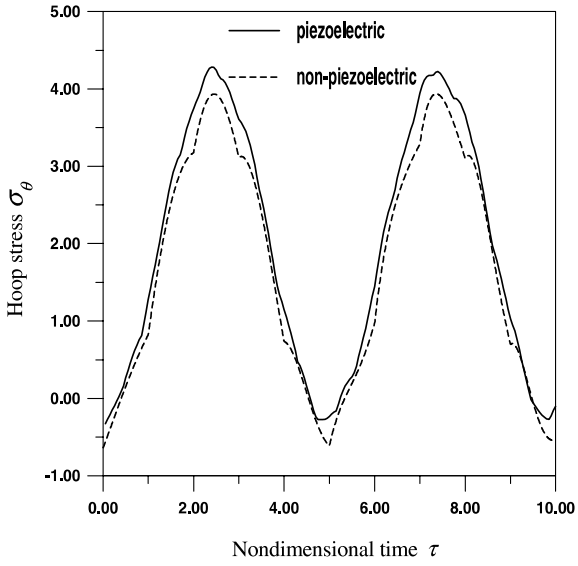

Fig. 2. History of dynamic stress σ_θ at $\xi = 0.5$.

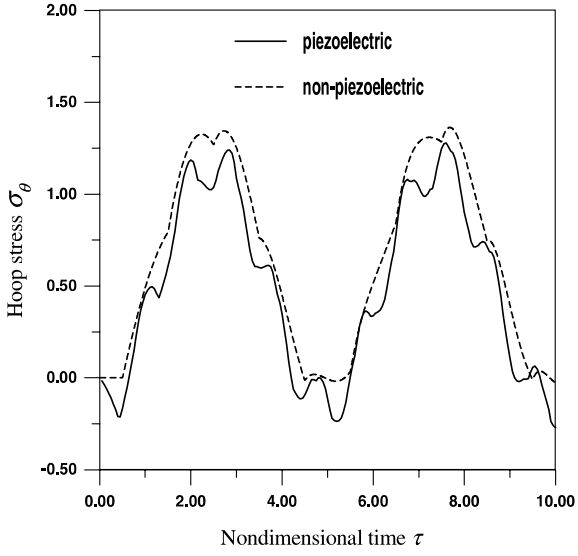

Fig. 3. History of dynamic stress σ_θ at $\xi = 1.0$.

appears in PZT-4 hollow cylinder, and the peak value is 3.93 times of the amplitude of the step input, less than that appears in PZT-4 hollow cylinder. We also notice that the responses of σ_θ in the PZT-4 are similar to that in the non-piezoelectric one.

Figs. 4 and 5 illustrate the responses of D at the different positions ($\xi = 0.5$, 0.75 and 1.0) and the distributions of ϕ at the different times ($\tau = 0.1$, 0.2 and 0.5) in the PZT-4 hollow cylinder subjected to a suddenly constant pressure on the internal surface. From Fig. 5 we find that the electric potentials at the

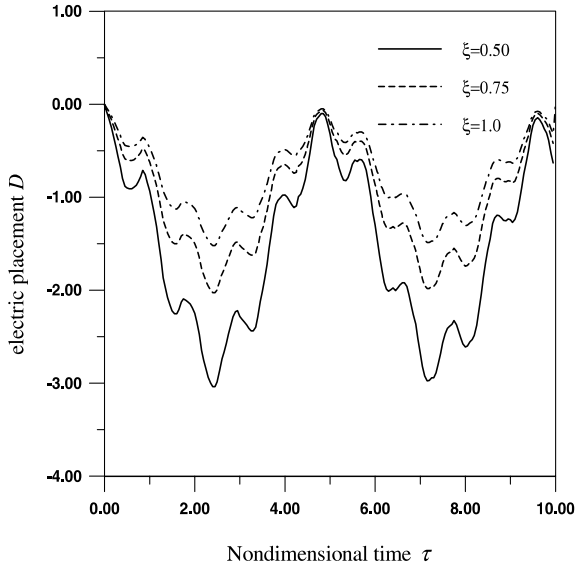

Fig. 4. Histories of dynamic electric displacement D at different locations.

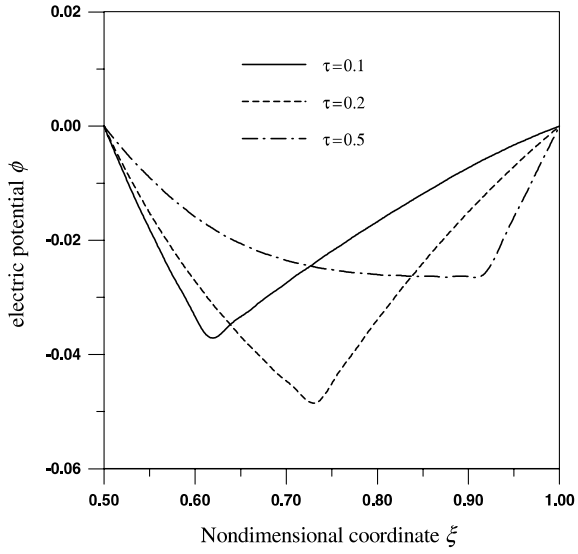

Fig. 5. Distributions of dynamic electric potential ϕ at different times.

internal and external surfaces keep zero. Thus the results satisfy the prescribed electric boundary conditions. So the correction of the numerical results is clarified.

Example 2. The transient responses in the hollow cylinder subjected to a sine time history pressure on the internal surface are to be considered. The boundary conditions are

$$p_a(\tau) = -\sigma_0 \sin(\omega_0 \tau), \quad p_b(\tau) = 0.0, \quad \phi_a(\tau) = 0.0, \quad \phi_b(\tau) = 0.0, \tag{63}$$

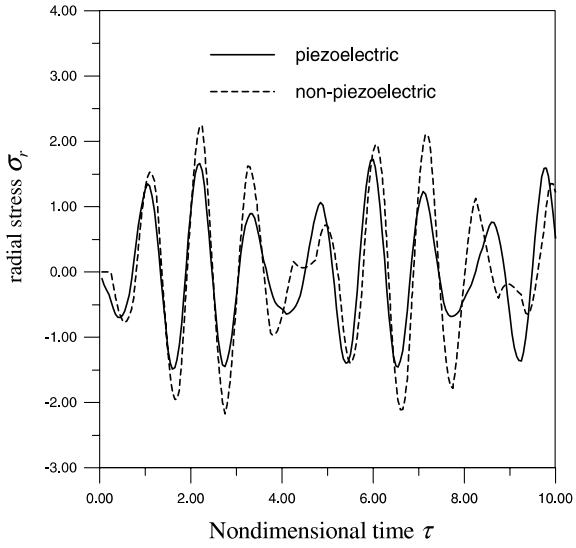

Fig. 6. History of dynamic stress σ_r at $\xi = 0.75$.

where ω_0 is the excitation frequency of the mechanical loads and we take $\omega_0 = 5.0$ and $\sigma_0 = 1.0$ for computation.

Fig. 6 shows the responses of σ_r at $\xi = 0.75$ (the middle surface) in the PZT-4 and non-piezoelectric hollow cylinder due to a sine time history pressure mechanical load on the internal surface. From the curves, we can see that the radial dynamic stress curves in the PZT-4 hollow cylinder are similar to those in the non-piezoelectric one. While the peak values of the curves of the PZT-4 hollow cylinder are less than those of the non-piezoelectric one.

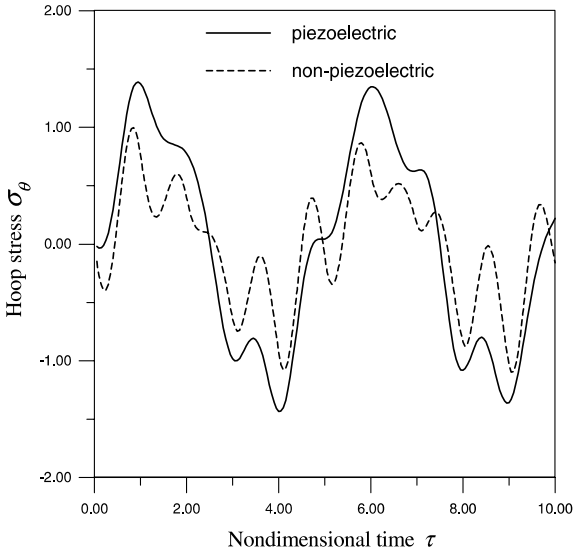

Fig. 7. History of dynamic stress σ_θ at $\xi = 0.5$.

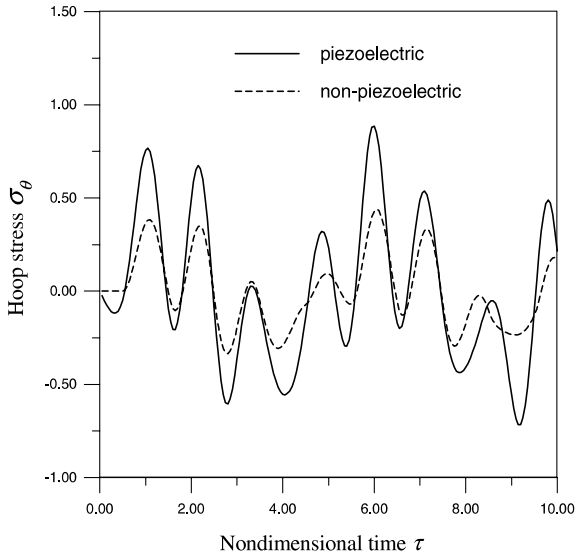

Fig. 8. History of dynamic stress σ_θ at $\xi = 1.0$.

Figs. 7 and 8 give the responses of σ_θ at $\xi = 0.5$ (the internal surface) and $\xi = 1.0$ (the external surface) in the PZT-4 and the non-piezoelectric hollow cylinder. From the curves, we find that the peak values of the dynamic hoop stresses in the PZT-4 hollow cylinder at $\xi = 0.5$ and 1.0 are lager than those in the non-piezoelectric one. We also notice that the responses of σ_θ in the PZT-4 are similar to those in the non-piezoelectric one.

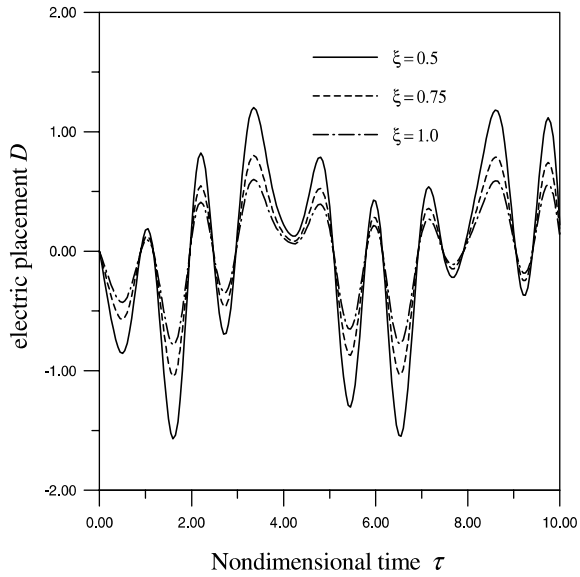

Fig. 9. Histories of dynamic electric displacement D at different locations.

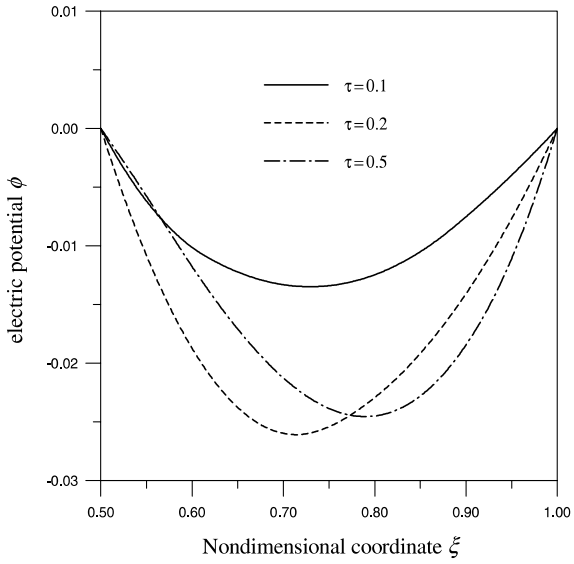

Fig. 10. Distributions of dynamic electric potential ϕ at different times.

Figs. 9 and 10 illustrate the responses of D at the different positions ($\xi = 0.5$, 0.75 and 1.0) and the distributions of ϕ at the different times ($\tau = 0.1$, 0.2 and 0.5) in the PZT-4 hollow cylinder. From Fig. 10, we find that the calculated electric potential at the internal and external surfaces satisfies the prescribed electric boundary conditions. So the correction of the numerical results is clarified in this respect.

Example 3. The transient responses of PZT-4 piezoelectric hollow cylinder subjected to a suddenly constant electric potential on the external surface are to be considered. The boundary conditions are

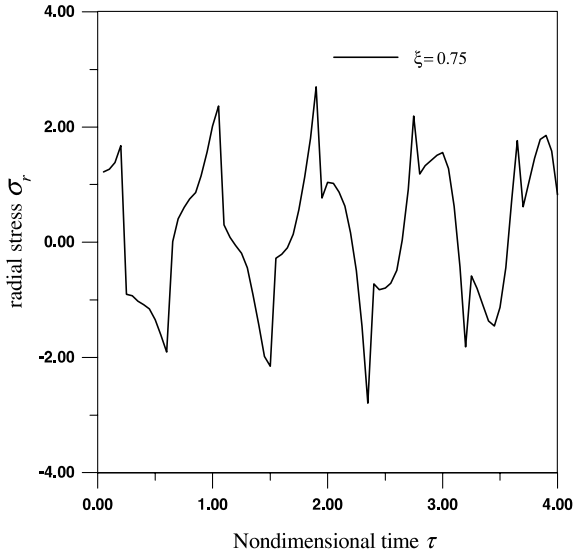

Fig. 11. History of dynamic stress σ_r at $\xi = 0.75$.

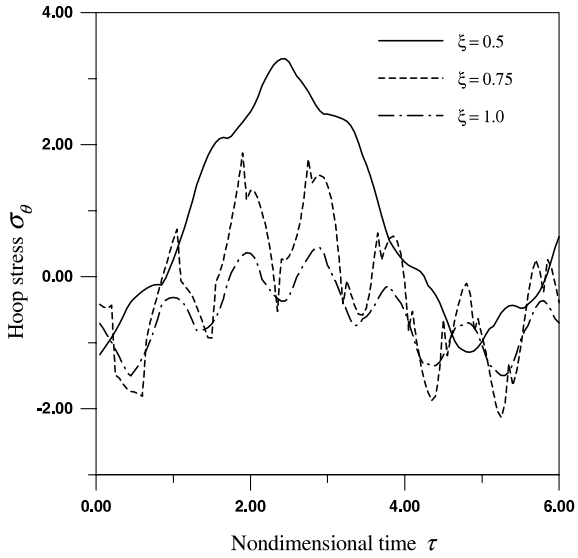

Fig. 12. Histories of dynamic stress σ_θ at different locations.

$$p_a(\tau) = 0.0, \quad p_b(\tau) = 0.0, \quad \phi_a(\tau) = 0.0, \quad \phi_b(\tau) = \phi_0 H(\tau), \tag{64}$$

where ϕ_0 is a prescribed constant electric potential and we take $\phi_0 = 1.0$ for computation.

Figs. 11 and 12 show the responses of σ_r and σ_θ in the PZT-4 hollow cylinder due to an external electric potential shock. By the computation, we find that the maximum values of σ_r appear at the inner part of the hollow cylinder but not at the internal or external surfaces. While the maximum values of σ_θ appear at $\xi = 0.5$ (the internal surface). Figs. 13 and 14 give the responses of D at the different positions ($\xi = 0.5$, 0.75 and 1.0) and the distributions of ϕ at the different times ($\tau = 0.1$, 0.2 and 0.5) in the PZT-4 hollow cylinder.

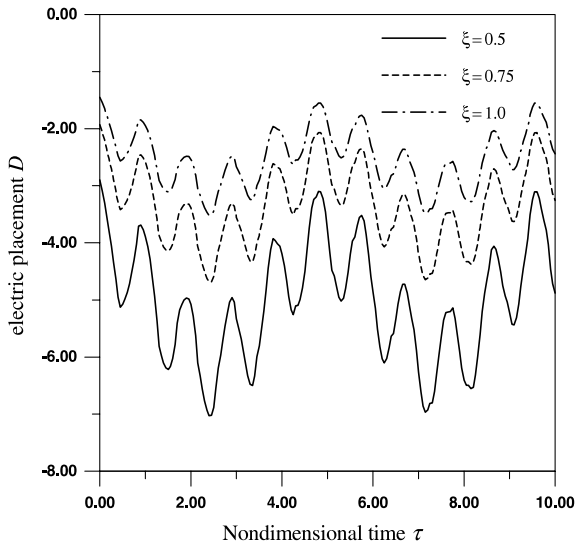

Fig. 13. Histories of dynamic electric displacement D at different locations.

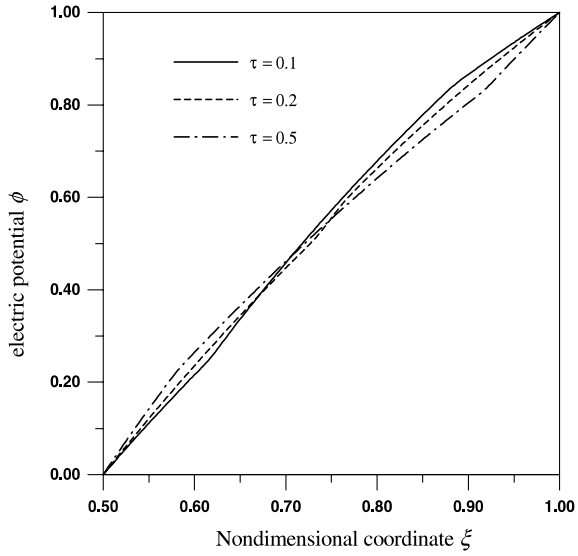

Fig. 14. Distributions of dynamic electric potential ϕ at different times.

From the curves, we notice that the maximum absolute value of D appears at the internal surface. The calculated electric potential also satisfies the prescribed electric boundary conditions.

Example 4. The transient responses of PZT-4 piezoelectric hollow cylinder subjected to a sine time history electric potential on the external surface are to be considered. The boundary conditions are

$$\begin{aligned} &p_a(\tau) = 0.0, \quad p_b(\tau) = 0.0, \\ &\phi_a(\tau) = 0.0, \quad \phi_b(\tau) = \phi_0 \sin(\omega_0 \tau), \end{aligned} \tag{65}$$

and we take $\phi_0 = 1.0$ and $\omega_0 = 5.0$ for computation.

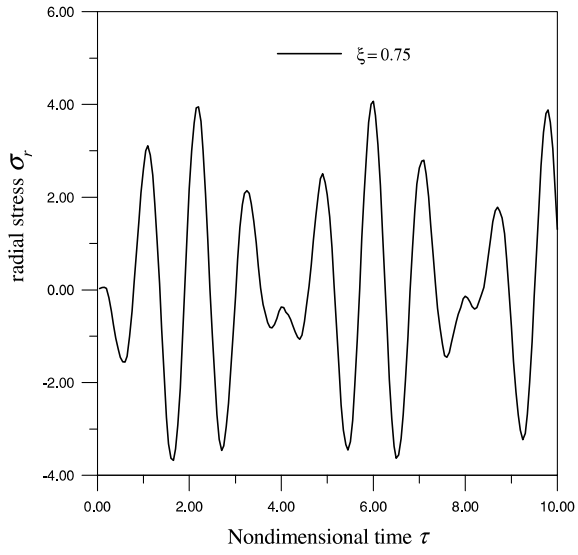

Fig. 15. History of dynamic stress σ_r at $\xi = 0.75$.

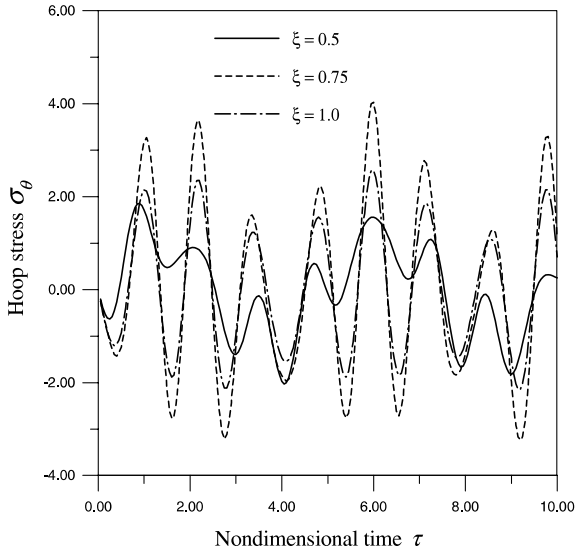

Fig. 16. Histories of dynamic stress σ_θ at different locations.

Figs. 15 and 16 depict the responses of σ_r and σ_θ in the PZT-4 hollow cylinder due to a sine time history electric potential on the external surface. By the computation, we find that the maximum values of σ_r and σ_θ appear at the inner part of the hollow cylinder but not at the internal or external surfaces. Figs. 17 and 18 give the responses of D at the different positions ($\xi = 0.5$, 0.75 and 1.0) and the distributions of ϕ at the different times ($\tau = 0.1$, 0.2 and 0.5) in the PZT-4 hollow cylinder. From Fig. 17, we notice that the maximum absolute value of D appears at the internal surface.

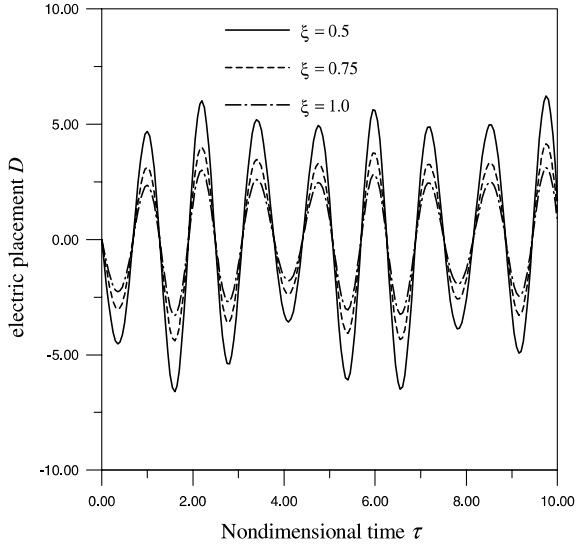

Fig. 17. Histories of dynamic electric displacement D at different locations.

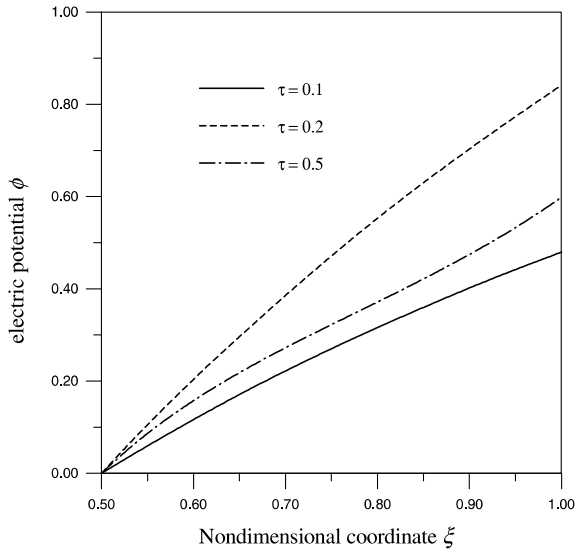

Fig. 18. Distributions of dynamic electric potential ϕ at different times.

5. Commentary

(1) If the electric boundary conditions in Eq. (9b) are expressed by electric displacements, we know only one boundary condition is needed. That is, if the electric displacement is prescribed on one surface, then the distributions of the electric displacement can be determined immediately by using Eq. (14). For this case, from the beginning to Eq. (47), the displacement solution has been obtained and the procedure of solving the integral equation is avoided. And the electric potential can be written as Eq. (50). But if we want to determine $\phi(\xi,\tau)$ completely, one boundary condition about ϕ must be known. That is, either $\phi_a(\tau)$ or $\phi_b(\tau)$ should be prescribed. The relationship between $\phi_a(\tau)$ and $\phi_b(\tau)$ is given in Eq. (52).

(2) If $\zeta_k(\tau)$ and $\eta_k(\tau)$ are polynomials of τ, then the integration in Eq. (60) can be expressed explicitly. So the computing accuracy can be improved. By using linear interpolation functions or high order interpolation functions, the well-results can be obtained efficiently. It is noted here that the recursion formula becomes very simply when linear interpolation functions are used. Particularly, the simplest recursion formula will be obtained when equal time step are used. Based on many kinds of test, we conclude that the satisfying numerical results can be obtained when $\Delta\tau \leqslant 0.05$.

Acknowledgements

The work was supported by the National Natural Science Foundation of China (no. 10172075) and Postdoctoral Foundation of China.

References

Adelman, N.T., Stavsky, Y., 1975. Axisymmetric vibration of radially polarized piezoelectric ceramic cylinders. Journal of Sound and Vibration 38 (2), 245–254.

Chou, P.C., Koenig, H.A., 1966. A unified approach to cylindrical and spherical elastic waves by method of characters. Journal of Applied Mechanics 33, 159–167.

Cinelli, G., 1966. Dynamic vibrations and stresses in elastic cylinders and spheres. Journal of Applied Mechanics 33, 825–830.

Ding, H.J., Chen, W.Q., Guo, Y.M., Yang, Q.D., 1997a. Free vibration of piezoelectric cylindrical shells filled with compressible fluid. International Journal of Solids and Structures 34, 2025–2034.

Ding, H.J., Guo, Y.M., Yang, Q.D., Chen, W.Q., 1997b. Free vibration of piezoelectric cylindrical shells. Acta Mechanica Solida Sinica 10, 48–55.

Dunn, M.L., Taya, M., 1994. Electroelastic field concentrations in and around inhomogeneties in piezoelectric solids. ASME Journal of Applied Mechanics 61, 474–475.

Kress, R., 1989. Linear Integral Equations, Applied Mathematical Sciences, vol. 82. Springer-Verlag World Publishing Corp.

Mcivor, I.K., 1966. The elastic cylindrical shell under radial impulse. Journal of Applied Mechanics 33, 831–837.

Rose, J.L., Chou, S.C., Chou, P.C., 1973. Vibration analysis of thick-walled spheres and cylinders. Journal of the Acoustical Society of America 53 (3), 771–776.

Sarma, K.V., 1980. Torsional wave motion of a finite inhomogeneous piezoelectric cylindrical Shell. International Journal of Engineering Science 18, 449–454.

Shul'ga, N.A., Grigorenko, A.Y., Loza, I.A., 1984. Axisymmetric electroelastic waves in a hollow piezoelectric ceramic cylinder. Prikladnaya Mekhanika 20 (1), 26–32.

Wang, X., Gong, Y.N., 1991. A theoretical solution for axially symmetric problem in elastodynamics. Acta Mechanica Sinica 7 (3), 275–282.